Hiroaki Date
Mem. ASME
e-mail: hdate@ssi.ist.hokudai.ac.jp

Satoshi Kanai
e-mail: kanai@ssi.ist.hokudai.ac.jp

Takeshi Kishinami
e-mail: kisinami@ssi.ist.hokudai.ac.jp

Graduate School of Information Science and Technology, Hokkaido University, Kita-14, Nishi-9, Kita-ku, Sapporo 060-0814, Japan

Ichiro Nishigaki
e-mail: ichiro.nishigaki.mp@hitachi.com
Hitachi, Mechanical Engineering Research Laboratory, 832-2, Horiguchi, Hitachinaka 312-0034, Japan

Takayuki Dohi
e-mail: t-dohi@hitachijoho.com
Hitachi Information Systems, 2-1-20 Jyonan, Mito 310-0803, Japan

High-Quality and Property Controlled Finite Element Mesh Generation From Triangular Meshes using the Multiresolution Technique

In this paper, we propose a new triangular finite element mesh generation scheme from various kinds of triangular meshes using the multiresolution technique. The proposed scheme consists of two methods: a mesh quality improvement method and a mesh property control method. The basic strategy of these methods is a combination of the mesh subdivision and simplification. Given mesh is first subdivided to obtain enough degree of freedom for a property change, then by simplification using edge collapse for the resulting mesh to change the mesh properties, we can easily improve and control the mesh properties required for finite element analysis. [DOI: 10.1115/1.2052847]

Keywords: Finite Element Analysis, Multiresolution Technique, Mesh Subdivision, Mesh Simplification, Quality Improvement, Property Control

1 Introduction

1.1 Background and Purposes. In product development, CAE using finite element analysis (FEA) is performed to evaluate the ability of designed shapes. For efficient product development, it is effective to perform FEA at the stage of the design as early as possible. One of the key issues to realizing this is the efficient mesh generation of product shapes, that is, it is desirable to generate high-quality meshes for FEA and to flexibly control the geometric and topological properties of the mesh required for efficient and accurate analysis.

Although much research on automatic mesh generation for FEA has been done, efficient mesh generation still remains a challenge. Usually, mesh generation for analysis is done by meshing a solid model using finite element meshers. The properties of the resulting meshes have relatively high quality, but the ability to efficiently control mesh properties is still insufficient, even in the commercial meshers, because remeshing of the solid model is always required individually when users need to have meshes with different properties.

To obtain the mesh of product shapes, other mesh generation methods are also available in the early design stage: for example, reverse engineering (RE) and simple tessellations. In RE, meshes are generated by triangulation of the unorganized points measured by a three-dimensional (3D) scanner or voxel data from computerized tomography. Simple tessellation generates the mesh by simply subdividing the surface of the solid model, and this function is commonly implemented in 3D-computer aided design (CAD) systems. In addition, the progress of archive of mesh data in a database allows us to reuse meshes generated by these approaches. However, the resulting meshes often include highly distorted triangles, and other properties of these meshes, such as valence and resolution (the number of faces) are not suitable for analysis. Therefore they cannot be directly applied to the analysis. Nevertheless, performing the analysis starting from such meshes is also required and effective for CAE during the early stages of design.

From these backgrounds, the requirements on the method for finite element mesh generation are summarized as follows: (1) it can generate high-quality mesh robustly, (2) it can control mesh property flexibly and efficiently, and (3) it can be applicable to a broad variety of meshes having different qualities and resolutions.

In this paper, we propose a new scheme for finite element mesh generation from triangular mesh using a multiresolution technique. The overview of our research is shown in Fig. 1. Our mesh generation scheme consists of two methods: a mesh quality improvement method and a mesh property control method. The basic strategy of these methods is a combination of two processes as shown in Fig. 2: a mesh subdivision process to obtain a high-density mesh from given mesh, and a mesh simplification process to change the mesh properties. Based on this strategy, in both of these methods, first, input meshes are converted to high-density mesh by the subdivision process (if necessary) to obtain the enough degree of freedom for property changes, and then mesh simplification with quality improvement or property control is applied to the high-density mesh. In the simplification process, the geometric and topological mesh properties such as geometric errors, valence of vertices, face shape quality, and face size can be improved and controlled corresponding to the user-specified mesh property conditions. Moreover, the multiresolution representation of the mesh is also obtained as a result of simplification, and the number of faces of the mesh can be progressively and easily increased or decreased. These methods and strategies allow us to use various kinds of meshes with various qualities and resolutions as input, and obtain high-quality and property-controlled mesh as

Contributed by the Engineering Simulation and Visualization Committee of ASME for publication in the JOURNAL OF COMPUTING AND INFORMATION SCIENCE IN ENGINEERING. Manuscript received October 9, 2004; final manuscript received March 2, 2005. Guest Editor: K. Shimada.

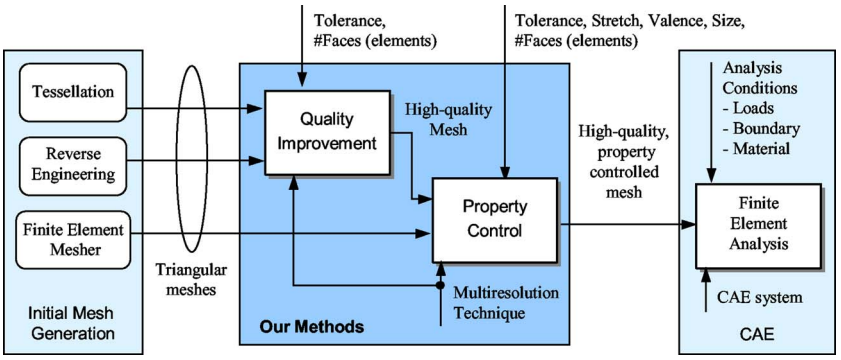

Fig. 1 An overview of our mesh generation scheme

output. In our research, we assume that the input meshes are limited to triangular meshes and 2-manifold ones without boundaries (conforming).

1.2 Related Works. For finite element mesh generation from solid models, the Delaunay, octree, and advancing front methods are becoming common [1,2], and many commercial systems for finite element mesh generation adopt these methods. As another effective mesh generation method, the bubble-meshing method was also proposed [3]. In our approach, meshes generated by these methods can be used as inputs, and the mesh properties, such as face size, face shape quality, valence, and geometric error are controlled in mesh simplification. The function for controlling all of these properties is not implemented in current finite element meshers. Moreover, these approaches always require solid models of the product shape; therefore the mesh cannot be used as input.

Several approaches for generating high-quality mesh from low-quality mesh have been developed. They are roughly classified into two types: mesh quality improvement based on local mesh modifications and remeshing using other domains of mesh. Methods for mesh quality improvement based on facet clustering, vertex insertions, and Delaunay triangulations were proposed [4,5]. These methods achieve robust high-quality mesh generation; however, explicit mesh property control is not considered and they cannot be applied to high-density meshes. In most remeshing methods, mesh parameterization is used for regularizing mesh connectivity and improving mesh quality [6,7], and a general approach for interactive remeshing was also proposed [8]. By using these remeshing methods, meshes with different properties can be obtained from a mesh by constructing parameterizations of the input mesh, defining new mesh in parameter domain, and by inverse mapping it into real space. As a result of such types of remeshing, certain multiresolution approaches and signal processing, such as using wavelets [9], could be applicable to the resulting meshes. However, for complex mechanical parts with small features and arbitrary genus, the definition of domain of parameterization is complex and the remeshing operation becomes difficult or inapplicable. Also, explicit geometric error control and sharp edge preservation are difficult to realize in these approaches. Another effective approach for remeshing proposed is based on geodesic distance [10]. This approach is very robust and the resulting mesh has better face shape quality, but mesh resolution (number of faces) and property control are not efficiently achieved.

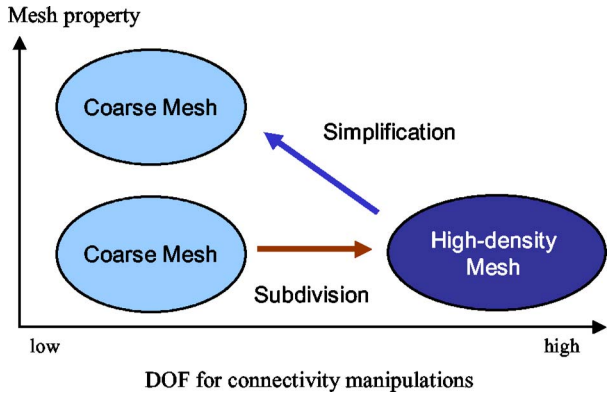

Fig. 2 Our mesh processing strategy

In our approach, mesh simplification and subdivision are applied to the meshes. Much research for mesh simplification has been conducted in the area of computer graphics [11–16], and these studies have become common and indispensable to many mesh applications. Their main purpose is to improve rendering speeds [11–13], to compress model data, to transfer data efficiently [14,16], and to reduce the cost of several geometric calculations [15]. These methods propose attractive mesh simplification from the aspects of fast computation, accurate geometric approximation, high visual fidelity in simplified mesh, and topological changes of the model. However, the quality or properties of mesh suitable for analysis could not be considered in these studies. In our method, we apply the mesh simplification approach to high-density meshes to generate high-quality and property controlled finite element mesh. Therefore, in contrast with existing simplification methods, the quality of mesh and the important properties for analysis of simplified mesh can be explicitly considered and controlled. For FE mesh generation, the method using the vertex removal based on a discrete envelope was also proposed [17]. This method including topological modification, such as hole filling, is effective for efficient FEA, however, quality improvement and explicit mesh property control was not discussed.

The effective use of subdividing triangular mesh has been developed to generate smooth surfaces. As the one of subdivision schemes for triangular meshes, the Loop subdivision scheme [18] is well known, and this method has been extended for several geometric modeling purposes [19]. In this approach, the given initial (control) mesh is uniformly subdivided. Then, vertex positions are modified based on a two-scale relationship of the basis functions of box splines. By contrast, our purpose in subdividing the mesh is to increase the degree of freedom for mesh connectivity manipulations in simplification. Therefore, we use simple nonuniform mesh subdivision based on selective midpoint insertions and uniform subdivision without changing the model shape.

We assume that the input meshes are conforming. If the solid model to be meshed is appropriate, i.e., it has no gap and no overlapping between surfaces, the conforming mesh can be obtained by simple tessellations and FE meshing of solid model using existing CAD system and CAE preprocessor. Even if nonconforming meshes are generated from them, the methods for making a mesh conform can be used [20]. For the nonconforming meshes obtained from RE, by using a similar stitching method

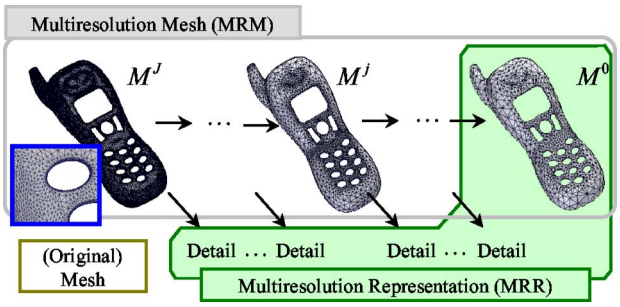

Fig. 3 Multiresolution representation and multiresolution mesh

[20], the mesh repairing method such as Ref. [21] or commercial RE data processing software, the conforming meshes can also be obtained.

The remainder of this paper is organized as follows: In Sec. 2, the basic concept of our research is described. The mesh property metrics used in our algorithm are shown in Sec. 3. Then, our mesh quality improvement method and property control method using mesh subdivision and simplification are described in Secs. 4 and 5. In Sec. 6, some examples and the effectiveness of our approaches are shown through visual and numerical evaluations. The conclusion of this paper is described in Sec. 7.

2 Basic Concept

2.1 Multiresolution Techniques. In this paper, we handle only triangular meshes. Triangular mesh represents the surface of a three-dimensional object by a set of triangle faces. We denote it by $M=\langle P,K\rangle$, where P shows a set of vertex coordinates: $P=\{\mathbf{p}_i=(x_iy_iz_i)^T\in R^3|1\leqslant i\leqslant n\}$, and K is the simplicial complex, which shows the topological connectivities of mesh elements: $K=V\cup E\cup F$, where vertices: $i\in V$, edges: $(i,j)\in E$, triangular faces: $(i,j,k)\in F$. The *multiresolution representation* (MRR) consists of the coarsest mesh and hierarchically decomposed details in mesh simplification. In some contexts [9], only hierarchical representation based on nested spaces, which requires subdivision connectivity in triangular mesh, are called as a multiresolution representation. In this paper, we use MRR to refer to the results of all methods for controlling the mesh resolution with mesh hierarchical representation. It can be obtained by iterative mesh simplification as shown in Fig. 3. By storing the MRR based on appropriate data structure, such as progressive mesh structure and multitriangulations [12,16], meshes with different resolutions can be reconstructed quickly. We call the resolution controllable meshes obtained from multiresolution representation *multiresolution meshes* (MRM), and also refer to the methods which can generate MRM as *multiresolution techniques*.

Several approaches to reduce the number of mesh elements were found [13], and are selectively used depending on the application purpose. In our method, the *edge collapse* operation [12] (EC: $(i,j)\rightarrow k$) as shown in Fig. 4 is adopted, because it can achieve successive resolution changes. It collapses an edge to a single vertex, and the inverse operation of this exists and is known as *vertex split*.

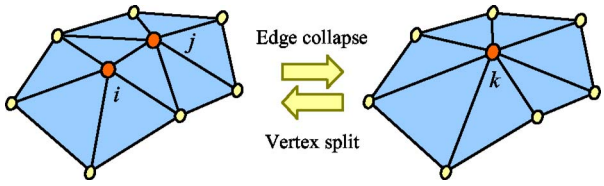

Fig. 4 Edge collapse and vertex split

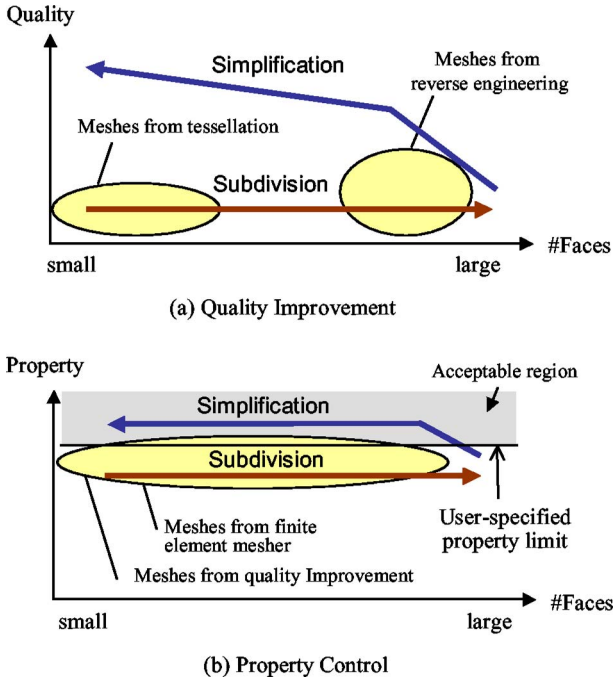

Fig. 5 Quality improvement and property control using subdivision and simplification

2.2 Basic Concept and Advantages. In our research, we focused on the following ability of high-density mesh and mesh simplification to realize robust and efficient mesh generation for analysis.

(a) High-Density Mesh. High-density mesh can easily be generated from any mesh by subdivision. It has a high-degree of freedom (DOF) for mesh connectivity manipulations within certain geometric tolerance. Here, connectivity manipulation means removing the vertex, edge, and face, and changing the connectivity of the mesh, such as edge swap operation. Also it can be obtained by using a finite element mesher robustly in comparison with a coarse one.

(b) Mesh Simplification. Using an appropriate data structure for storing the lost details in simplification, fast and efficient control of the number of faces of the mesh can be achieved. It also has the potential ability to change the other properties of mesh because there is high-flexibility of algorithm design, such as the operations for reduction of the number of faces and the definition of simplification priorities [13]. Moreover, its operation is very robust.

According to the requirements for finite element mesh generation described in Sec. 1.1, it is effective to generate several finer meshes from high-density meshes through mesh simplification. Therefore, in our approaches, we first generated the high-density mesh by subdivision to increase the DOF for connectivity manipulation, then by applying mesh simplification, we could realize mesh quality improvement and mesh property control, respectively. As shown in Fig. 5, these strategies enable us to process various kinds of meshes with different qualities and resolutions as input. In our quality improvement method, we designed the simplification method so as to improve the face shape quality within the user-specified tolerance, as shown in Fig. 5(*a*). In the property control method, the quality of mesh is preserved and the resulting meshes satisfy user-specified property control parameters, as shown in Fig. 5(*b*).

The advantages of our approach are summarized as follows.

(a) Broad range of applicableness. Starting mesh quality improvement and property control from high-density mesh allows us to apply them to any (2-manifold) triangular meshes obtained from tessellation of CAD models, meshing using a finite element

mesher and reverse engineering by 3D scanner or computerized tomography, because they can easily be converted to high-density mesh.

(b) Flexible and efficient mesh property control. Our approach can explicitly control the triangular face size, face shape quality, valence and geometric errors by specifying mesh property control parameters. Therefore, the user can obtain a mesh suitable for their purposes and computing environments for analysis. Moreover, as a result of our mesh generation method, a multiresolution representation of input high-density mesh is obtained. Using MRR, we can also change and control the number of triangular faces quickly and successively.

(c) Robust mesh generation. The mesh subdivision and simplification process only consists of very simple operations for the mesh model, and is very robust independent of shape complexities. Therefore, our approach can certainly generate high-quality property controlled meshes for analysis.

3 Mesh Property Metrics

In our algorithm, three property metrics are used to evaluate the geometric errors in simplification, face size, and face shape quality, respectively. The following are the metrics for evaluating such mesh properties. We omitted the description of the metrics of other two properties that are also considered in our algorithm, i.e., valence and the number of triangular faces, because their evaluations are obvious.

3.1 Geometric Errors in Simplification. The geometric error caused by applying edge collapse $(i,j)\rightarrow k$ is evaluated using the method of Garland and Heckbert [11]. This error represents the sum of squared distances between the new vertex position $\mathbf{p}_k$ and the planes, which are defined by triangular faces connected to vertices i,j. The error $d_{ij}(k)$ for an edge (i,j) can be written as follows:

$$d_{ij}(k)=\mathbf{p}_k^T(\mathbf{A}_i+\mathbf{A}_j)\mathbf{p}_k+2(\mathbf{B}_i+\mathbf{B}_j)\mathbf{p}_k+C_i+C_j \tag{1}$$

where $\mathbf{A}_i=\Sigma_{f\in f^*(i)}\mathbf{n}_f\mathbf{n}_f^T$, $\mathbf{B}_i=-\Sigma_{f\in f^*(i)}(\mathbf{n}_f^T\mathbf{p}_i)\mathbf{n}_f^T$, and $C_i=\Sigma_{f\in f^*(i)}(\mathbf{n}_f^T\mathbf{p}_i)^2$. The vector $\mathbf{n}_f$ shows the unit normal vector of the triangular face f, and $f^*(i)$ indicates the set of triangular faces connected to vertex i. We call the matrices and scalar value $\mathbf{A}_i,\mathbf{B}_i,C_i$, which are defined on each vertex in mesh as *error evaluation indices*.

In finite element mesh, it is important to preserve sharp edges; therefore, we extended the error evaluation indices so that they evaluated the point-to-line squared distances too. Similar considerations to Garland's method, the extended error evaluation indices, which can also evaluate the sum of squared distances between the point and lines constructing sharp edges, can be formulated as follows:

$$\hat{\mathbf{A}}_i=\mathbf{A}_i+w_e\sum_{e\in\hat{e}^*(i)}\begin{pmatrix}1-d_{ex}^2 & -d_{ex}d_{ey} & -d_{ex}d_{ez}\\ -d_{ex}d_{ey} & 1-d_{ey}^2 & -d_{ey}d_{ez}\\ -d_{ex}d_{ez} & -d_{ey}d_{ez} & 1-d_{ez}^2\end{pmatrix} \tag{2}$$

$$\hat{\mathbf{B}}_i=\mathbf{B}_i+w_e\sum_{e\in\hat{e}^*(i)}(-\mathbf{p}_i+(\mathbf{d}_e^T\mathbf{p}_i)^2\mathbf{d}_e)^T \tag{3}$$

$$\hat{C}_i=C_i+w_e\sum_{e\in\hat{e}^*(i)}(\mathbf{p}_i^T\mathbf{p}_i+(\mathbf{d}_e^T\mathbf{p}_i)^2) \tag{4}$$

where $\mathbf{d}_e=(d_{ex}d_{ey}d_{ez})^T$ shows the unit direction vector of an edge e, and $\hat{e}^*(i)$ is a set of edges on the sharp edge and connected to the vertex i. Scalar value w_e is a weight to control the strength of sharp edge preservation. By substituting $\hat{\mathbf{A}}_i,\hat{\mathbf{B}}_i,\hat{C}_i$ for $\mathbf{A}_i,\mathbf{B}_i,C_i$ and by performing error evaluation using Eq. (1) (and new vertex position calculation in Secs. 4 and 5), sharp edges can be well preserved. In simple implementation, we can identify the sharp edge by evaluating dihedral angles using the inner product of the unit normal vectors of two connected faces, and this is useful for the meshes resulting from simple tessellations or FE meshing of solid models. However, for the meshes resulting from 3D scanning, it is not effective because they have small bumps from the scanning noise. In this case, we can use several feature edge detection methods, such as the one based on normal voting [22]. Our edge preservation approach can be applied to the sharp edges resulting from such feature edge detection methods. The weights w_e can be determined according to sharpness (to be larger for the sharper edges).

3.2 Face Size. The *size* of a triangular face in the mesh is defined as the longest edge length of the triangular face f, and is denoted by

$$Sz(f)=\max_{e\in e^*(f)}l_e \tag{5}$$

where l_e is the length of the edge e, $e^*(f)$ is a set of edges adjacent to a triangular face f.

3.3 Face Shape Quality. The shape quality of a triangular face is evaluated using the *stretch*, which is one of the measures of face shape quality used in the CAE area. Stretch is defined as the product of $\sqrt{12}$ and the radius of the inscribed circle of the triangular face divided by the longest side length of the face. Stretch is calculated by

$$St(f)=\frac{\sqrt{12}}{\max\limits_{e\in e^*(f)}l_e}\sqrt{\frac{\prod\limits_{e\in e^*(f)}(s-l_e)}{s}} \tag{6}$$

where s is half of the sum of three edge lengths of a triangular face. The value of $St(f)$ is 1 for an equilateral triangle and decreases gradually for distorted triangles. Finally, the value of stretch becomes zero for the degenerate triangle. Faces (elements) with a stretch larger than 0.2 are recommended for analysis of triangular mesh [23].

4 Mesh Quality Improvement

In our mesh quality improvement, we assume that the input of our algorithm is the low-quality coarse mesh, as shown in Fig. 5. Such meshes are often obtained by tessellation of solid models. If the input mesh has high density, which may often be obtained by reverse engineering, we can skip the subdivision process in Sec. 4.1 and simply apply mesh simplification with quality improvement as described in Sec. 4.2 to the input mesh. In mesh quality improvement, the user specify two parameters σ_{SZ} and τ_{TL}. These can control the degree of subdivision and geometric tolerance in simplification. As a result of this method, quality-improved coarse meshes are obtained from MRR.

4.1 Mesh Subdivision for Quality Improvement. To effectively improve mesh quality by simplification based on edge collapse, it is necessary to increase the degree of freedom of mesh connectivity manipulation by mesh subdivision, because a lower number of edge collapse operations may not achieve enough quality improvement. Although several approaches to mesh subdivision are useful for such a purpose, we used selective midpoint insertions to the edges and face subdivisions using the inserted midpoints. It is applicable locally and can make the size of faces uniform. As a result, the number of triangular faces increases, but the shape of the mesh model remains unchanged.

First, the midpoints are inserted into the edges, whose lengths are longer than the user specified threshold value σ_{SZ}, which is called the *subdivision parameter*. Then, according to the mesh subdivision rules shown in Fig. 6, the triangular faces are subdivided. By repeating these midpoint insertions and face subdivisions until the lengths of all edges become shorter than σ_{SZ}, low-quality dense mesh, which has enough degree of freedom for topological connectivity manipulation, can be obtained. The selec-

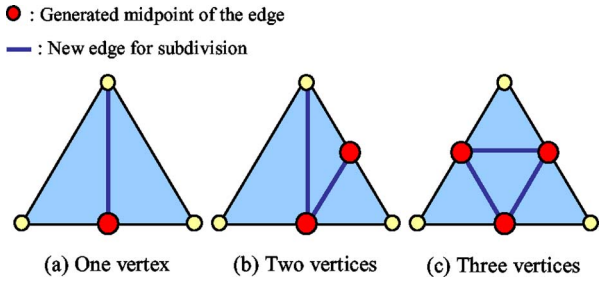

Fig. 6 Mesh subdivision rules

tion of the appropriate value of σ_{SZ} is discussed in Sec. 6.1.

4.2 Mesh Simplification for Quality Improvement. By applying an iterative edge collapse operation with quality improvement to the resulting subdivided high-density mesh, high-quality coarse or resolution controllable mesh can be generated. Mesh simplification consists of the following four steps, as shown in Fig. 7.

Step 1. New vertex position calculation. For all edges (or edges modified by edge collapse), the new vertex positions for edge collapse are calculated (*A*-1).

Step 2. Valid edge extraction. All edges (or edges modified by edge collapse) are checked for whether edge collapse can be applied or not (*A*-2). The edges satisfying the user-specified parameters are identified as *valid edges*, and become candidates for edge collapse. If there are no valid edges, the algorithm terminates.

Step 3. Priority index calculation. For each valid edge, the priority index for determining the order of edge collapse operations is calculated (*A*-3).

Step 4. Edge collapse. Edge collapse is applied to edges with the largest priority index (*A*-4), then return to step 1.

In step 2, the user specified tolerance can be guaranteed, and by defining the priority index appropriately to evaluate the degree of mesh quality improvement in step 3, high-quality coarse mesh can be obtained through a mesh simplification process. By storing the collapsed edge and neighbor information based on appropriate data structure, such as progressive mesh structure and multitriangulations [12,16], the MRR of input meshes can be obtained, therefore meshes with different resolution can be reconstructed quickly.

4.2.1 New Vertex Position Calculation. The position of the new vertex $\mathbf{p}_k$ for the edge collapse $(i,j)\rightarrow k$ is calculated for each edge of the mesh. In our approach, two positions are adopted as candidates. The first is the centroid of neighboring vertices of i and j, which can preserve the triangular face shape quality well. The second is the vertex position that minimizes the geometric error defined by Eq. (1). This position can be determined by $\mathbf{p}_k = -(\mathbf{A}_i+\mathbf{A}_j)^{-1}(\mathbf{B}_i+\mathbf{B}_j)^T$ [11]. One of them is sequentially selected according to the evaluation results of valid edge extraction described in the next section.

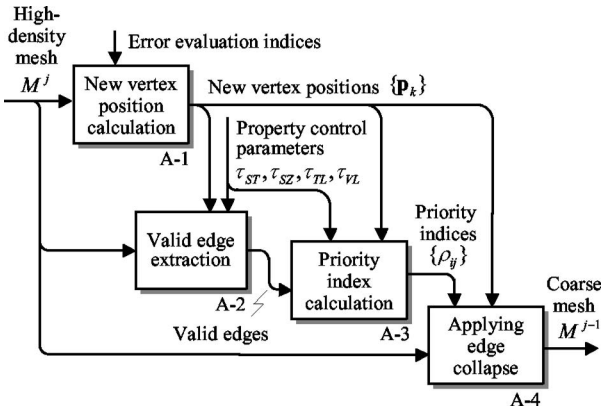

Fig. 7 Mesh simplification algorithm

4.2.2 Valid Edge Extraction. Each edge is checked to evaluate whether or not the local mesh near the edge satisfies the user-specified simplification parameter τ_{TL}, which represents the tolerance of the approximation, after the edge collapse operation. The edges, which satisfy the condition $d_{ij}(k)\leqslant\tau_{TL}$ are identified as valid edges. They can be candidates for edge collapse. Furthermore, by evaluating the change of direction of the normal vectors of triangular faces before and after the edge collapse operation, mesh foldover is checked [11,13]. If mesh foldover occurs, the corresponding edge can be removed from a set of valid edges.

4.2.3 Priority Index Calculation and Edge Collapse. In our method, we define the priority index so that its value for the edge with a high-degree of improvement of face shape quality and uniformity of face size after the edge collapse operation becomes large.

First, the metric of face shape quality improvement in edge collapse operations for all edges is defined. Edge collapse removes the two triangular faces sharing the edge (i,j), and other faces connected to the vertices i and j still remain and are modified. Therefore, the degree of face shape quality improvement Δq_{ij} can be evaluated as the ratio of the face shape quality of the local faces before and after edge collapse

$$\Delta q_{ij} = \frac{q(\hat{f}^*(i,j))}{q(f^*(i,j))} \tag{7}$$

where $q(F)$ shows the face shape quality of a set of triangular faces F, and here we assume that it takes a larger value for a higher quality. $f^*(i,j)$ and $\hat{f}^*(i,j)$ show the triangular faces connected to the vertices i, j and vertex k. Several choices of q can be considered to define the quality of a set of triangular faces. We use the products of the average and the minimum stretch formulated by

$$q(F) = \frac{1}{|F|}\min_{f\in F} St(f) \Sigma_{f\in F} St(f) \tag{8}$$

where $|F|$ is the number of triangular faces in a set of faces F. A larger Δq_{ij} means that the corresponding edge (i,j) has an extremely distorted triangle or a larger distortion of triangles on average in its neighborhoods, and by applying edge collapse operation to it, the mesh quality can be improved more.

Mesh simplification generally enlarges the size of the triangular faces. Therefore, for uniformity of the face sizes, the measure Δq_{ij} is weighted by the inverse of the average of the normalized size of the triangles connected to the edge (i,j), which can be represented by $s_{ij}=|\hat{f}^*(i,j)|/\Sigma_{f\in f^*(i,j)} Sz(f)$. The final priority index ρ_{ij} of the edge (i,j) can be calculated by $\rho_{ij}=s_{ij}\times\Delta q_{ij}$ for each edge. Finally, the edge collapse is applied to the edge with the largest priority index.

5 Mesh Property Control

In our mesh property control, we assume that the input of our algorithm is high-quality coarse mesh. Our method, other quality improvement methods or finite element meshers often generate such meshes as shown in Fig. 5. If the input mesh has a high-density, which may be obtained by a finite element mesher in a certain setting of parameters for the size, we can also skip the subdivision process in Sec. 5.1 and apply only the simplification with property control described in Sec. 5.2 to the input mesh. The subdivision is performed using a user-specified number of subdivision operations to generate high-quality dense mesh, and mesh simplification simultaneously reduces the number of mesh ele-

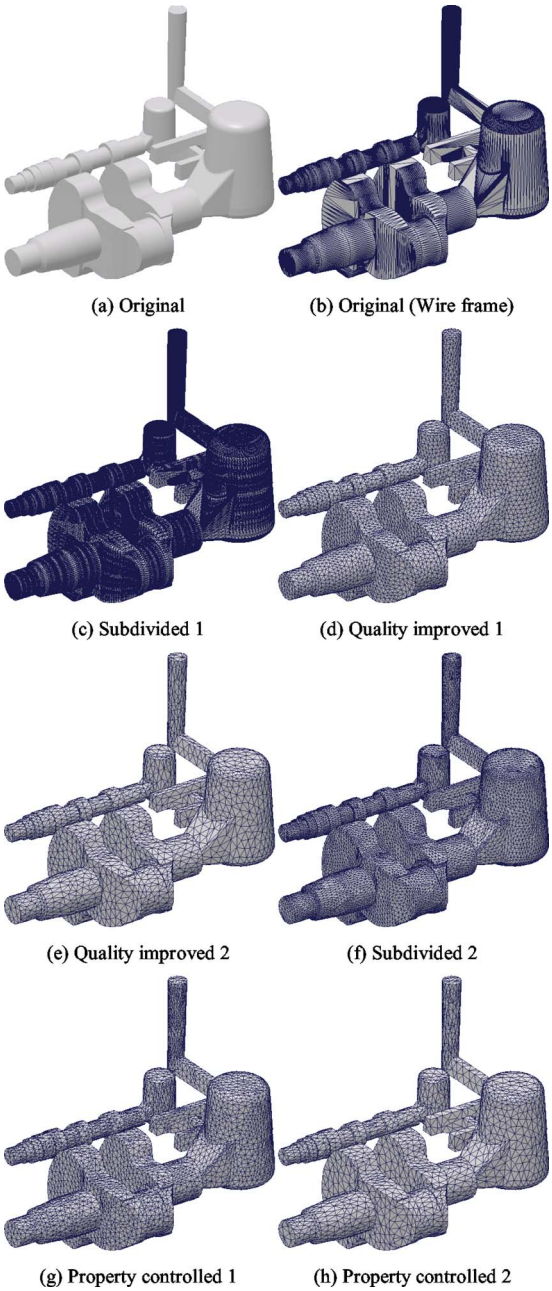

Fig. 8 Results for crankshaft mesh generated by tessellation

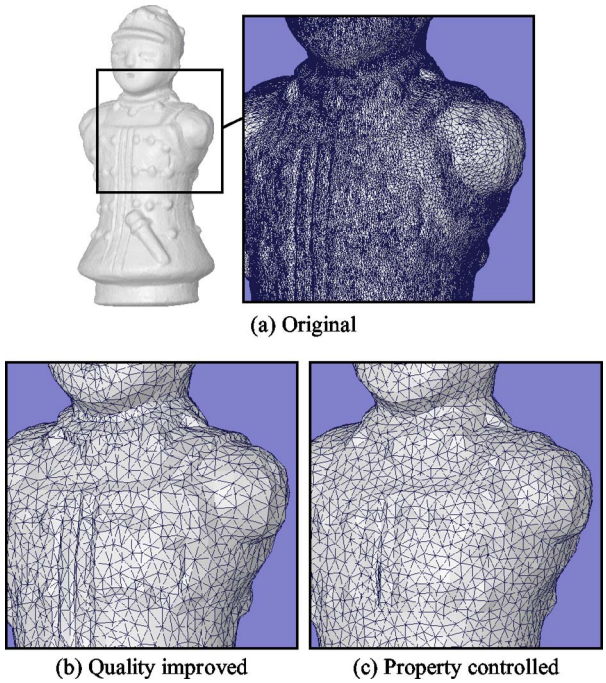

Fig. 9 Results for terra cotta mesh generated by reverse engineering

ments, preserves mesh quality, and controls the mesh properties using user-specified property control parameters, which represent the upper and lower limits for mesh property metrics. As a result of this method, the high-quality MRM satisfying the user-specified property conditions for geometric error, face shape quality, size, and valence is obtained.

5.1 Mesh Subdivision for Property Control. Similar to the method for mesh quality improvement described in Sec. 4.1, subdivision is applied to the input mesh to increase the DOF for connectivity manipulations. In our setting, the input mesh is high quality, and the high-quality dense mesh is required as a result of subdivision. Subdivision using selective midpoint insertions, as described in Sec. 4.1, generates dense mesh with uniform face size, but it also causes a decrease of quality; therefore, we cannot use such a subdivision method. Fortunately, our problem settings for the quality of input mesh allow us to adopt one-to-four uniform subdivision as shown in Fig. 6(*c*), because this type of subdivision generates four similar triangles to the original one, i.e., qualities of face shape are unchanged. In our method, first the user specifies the number of subdivisions and then the system performs the one-to-four mesh subdivision according to the number of times specified by the user. As a result, the number of triangular faces becomes four times in one step subdivision. Therefore, we can also specify the approximate target number of triangular faces.

5.2 Mesh Simplification for Property Control. The basic algorithm of simplification is the same as the one for quality improvement, as shown in Fig. 7. Also, the schemes for new vertex position calculation (*A*-1 in Fig. 7) and the rule for determining the order of the edge collapse operation (*A*-4 in Fig. 7) described in a previous section can be straightforwardly used. To achieve high-quality and property controlled mesh generation, it is enough to impose additional constraints for satisfying other property control parameters in the valid edge extraction phase, and to modify the priority index in its calculation phase so as to preserve face shape quality well.

5.2.1 Valid Edge Extraction. All edges are checked for whether or not the local mesh near the edge satisfies the user-specified mesh property control parameters after the edge collapse operation. The edges are identified as valid when they satisfy the following conditions:

(a) Satisfaction of geometric tolerance:

$$d_{ij}(k) \leqslant \tau_{TL}$$

(b) Satisfaction of the lower limit of face shape quality:

$$\forall f \in f^*(k);\ St(f) \geqslant \tau_{ST}$$

(c) Satisfaction of the upper limit of the face size:

$$\forall f \in f^*(k);\ Sz(f) \leqslant \tau_{SZ}$$

(d) Satisfaction of the upper limit of the number of valence:

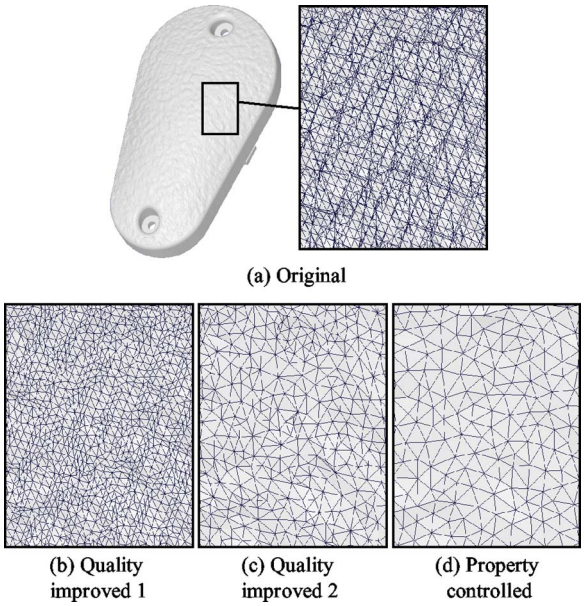

Fig. 10 Mesh quality improvement for textured mouse generated by mesh combining

$$|v^*(i)| + |v^*(j)| - 4 \leq \tau_{VL}$$

where $v^*(i)$ shows a set of the neighboring vertices of the vertex i. Note that the vertex k is the one generated from edge collapse for the edge (i,j), and evaluations for $f^*(k)$ can be done for the new faces connected to vertex k, which are created temporarily using vertex k. Similar to the method in Sec. 4.2, by evaluating the change of directions of the face normals, we avoid mesh foldover.

In these settings, we assume that the input high-density mesh satisfies the upper limit of triangular face size and valence τ_{SZ}, τ_{VL}, and the lower limit of face shape quality τ_{ST}. Upper limits can be mostly satisfied in the mesh from finite element meshers and quality improvement methods. However, the mesh generated from such methods often does not satisfy this condition (b). In such a case, for satisfying the lower limit of stretch τ_{ST}, only edges which do not satisfy condition (b) are collapsed until all triangular faces satisfy the τ_{ST} in the first step of mesh simplification.

5.2.2 Priority Index Calculation and Edge Collapse. The priority index, which shows the priority of edge collapse applications, is calculated for each valid edge. We define the priority index so that the edge with a larger index has a higher degree of face shape quality preservation and uniformity of face size. The priority index ρ_{ij} for the valid edge (i,j) can be described as

$$\rho_{ij} = \frac{1}{2(|f^*(k)| - 1)} \left\{ \sum_{f \in f^*(i) \cup f^*(j)} \frac{\tau_{SZ}}{Sz(f)} \times \min_{f \in f^*(k)} St(f) \times \sum_{f \in f^*(k)} St(f) \right\} \tag{9}$$

In Eq. (9), the first term in a brace shows the sum of the ratios between the size of triangular face and user-specified maximum size in current local mesh. The second and third terms represent the minimum and the sum of stretches of newly generated faces by collapsing the edge (i,j). If we apply the edge collapse to the edge (i,j) with larger ρ_{ij}, then we can obtain local mesh with higher quality in coarse mesh. Therefore, edge collapse is applied to the edge with the largest priority index ρ_{ij}.

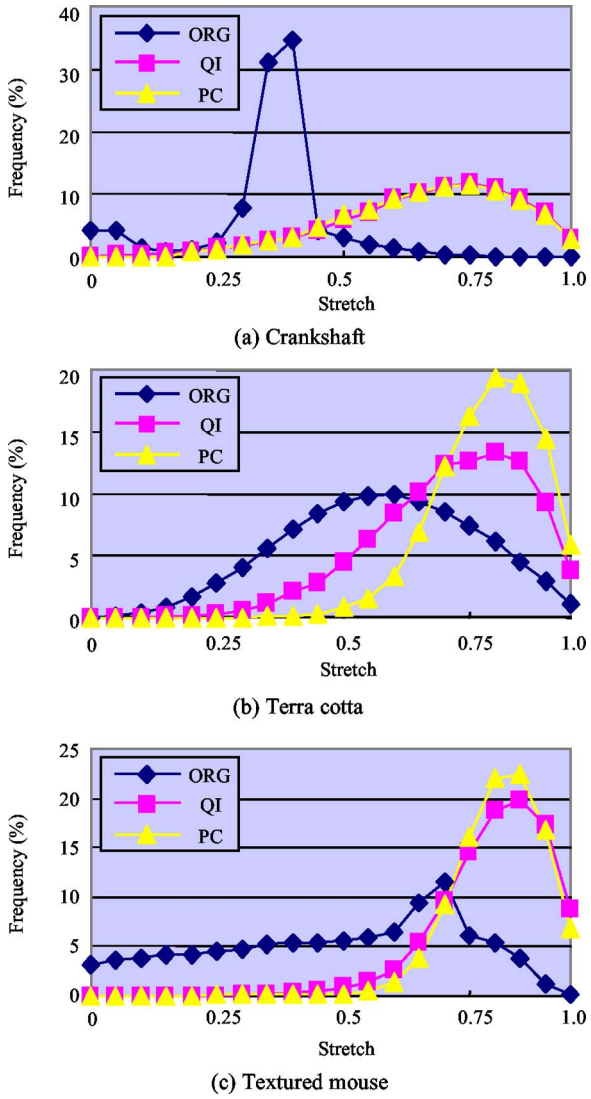

Fig. 11 Stretch distributions

6 Results and Discussions

6.1 Resulting Meshes. The meshes generated by applying the proposed quality improvement and property control methods to several kinds of meshes are shown in Figs. 8–10. The dimensions and number of triangular faces of each model are shown in Table 1.

The resulting meshes of the proposed method for the input mesh of a crankshaft generated by tessellation of a 3D solid model in a CAD system are shown in Fig. 8. In Fig. 8, (a) and (b) show the original mesh, (d),(e) and (g),(h) are the quality improved meshes and property controlled meshes, respectively. Intermediate meshes resulting from subdivisions are shown in Figs. 8(c) and 8(f). By comparing the meshes shown in Figs. 8(b) and 8(d),(e), it can be observed that the quality and size uniformity of triangular faces is improved. Figure 9 shows the results for the mesh generated by reverse engineering. The input mesh in this example has low quality and high density. Similar to the previous result, high-quality and coarse mesh could be obtained from low quality dense mesh.

In the mesh morphing or geometric texture integration approach based on mesh parameterization [24,25], the topological elements of two or more meshes are often combined to accurately represent the interpolated or detailed shapes. Generally, the resulting combined mesh has many extremely distorted and small triangular

Table 1 Mesh information, used parameters and quality[a]

Mesh (generation tool of original)	Dimension	State[b]	No. of faces	Stretch Ave.	Stretch Min	Valence max	Size max
Crankshaft (tessellation)		ORG	65,140	0.373	0.000	69	229.767
	Height 232.0	SBD1	266,484	0.197	0.000	74	(8) 8.000
	Width 398.0	QI2	7,500	0.689	0.024	10	31.863
	Depth 516.5	SBD2	30,000	0.689	0.024	10	15.931
		PC2	7,500	0.688	(0.2) 0.202	(10) 10	(20) 19.999
Terra cotta (reverse engineering)		ORG	203,174	0.595	0.011	13	11.105
	Height 162.4	SBD1	…	…	…	…	…
	Width 83.7	QI	10,000	0.737	0.077	11	7.938
	Depth 75.9	SBD2	40,000	0.737	0.077	11	3.969
		PC	10,000	0.812	(0.2) 0.259	(11) 9	(5) 4.974
Textured mouse (mesh combining)		ORG	192,222	0.511	0.000	17	51.442
	Height 26.1	SBD1	374,990	0.414	0.000	24	(1) 1.000
	Width 56.0	QI2	40,000	0.824	0.074	10	2.968
	Depth 100.0	SBD2	160,000	0.824	0.074	10	1.484
		PC	40,000	0.833	(0.2) 0.216	(10) 10	(2) 1.703

[a]Values in parentheses are user-specified parameters in mesh generation.
[b]ORG: original, SBD: subdivided, QI: quality improved, PC: property controlled.

faces. Our mesh simplification approach with quality improvement was able to reduce the number of such faces efficiently, as shown in Fig. 10. From Figs. 10(*a*) and 10(*b*), we can see that mesh simplification is first performed near the region with highly distorted and small triangular faces.

Figure 11 shows the stretch distributions of the resulting meshes. The evaluations of the minimum and average of stretch, max size and valence are shown in Table 1. Parentheses in the table denote the user-specified property control parameters. From these results, it was confirmed that our approach was able to stably improve the face shape quality regardless of the kinds of the input meshes. Moreover, Table 1 shows that the property controlled meshes satisfy the user-specified property control parameters. The meshes generated by different tolerance settings are shown in Fig. 12. We can see that the geometric errors in simplified mesh are controlled by user-specified tolerances. The tolerances τ_{TL} used for the examples in Figs. 8–10 were 1.0, 2.0, and 0.1, respectively.

Based on evaluations for several meshes in different quality improvement parameter settings (σ_{SZ}, τ_{TL}), the following were observed: the use of a subdivision parameter σ_{SZ} similar to the target face size can produce mesh with better quality. There is a trade-off relationship between the simplification parameter τ_{TL} and quality. A small simplification parameter causes less of a reduction of the number of triangular faces. The simplification parameter has to be adjusted and determined interactively by the user according to the uses of the resulting mesh.

6.2 Comparison. Figures 13 and 14 show the resulting meshes of our approach and meshes generated from commercial

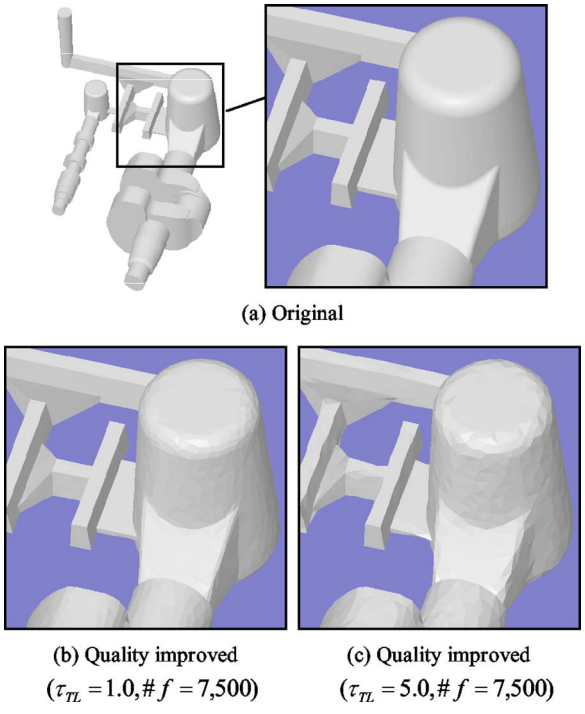

Fig. 12 Tolerance control

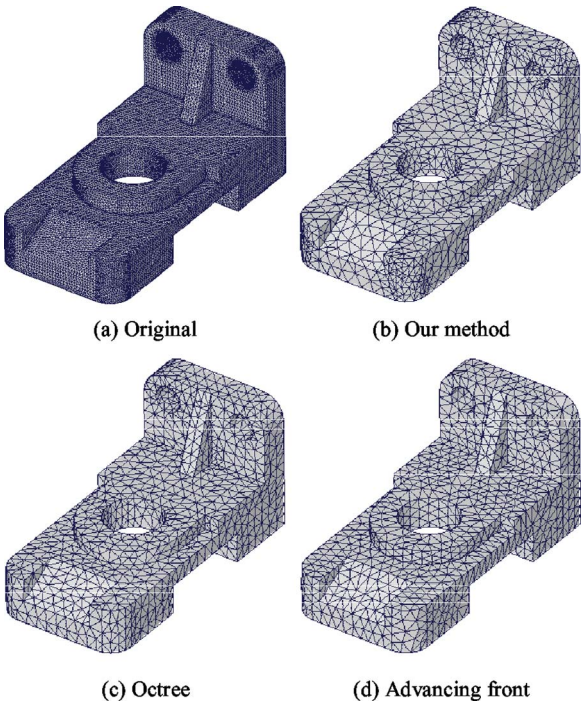

Fig. 13 A comparison with finite element meshers for a mechanical part

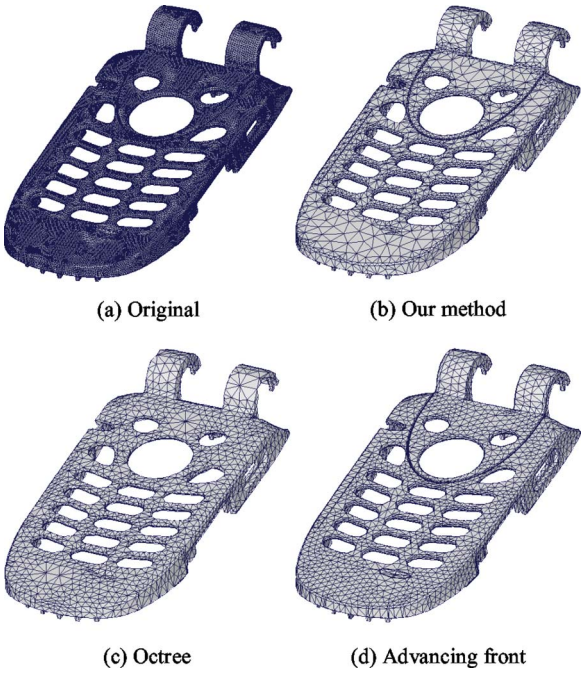

Fig. 14 A comparison with finite element meshers for a cellular phone

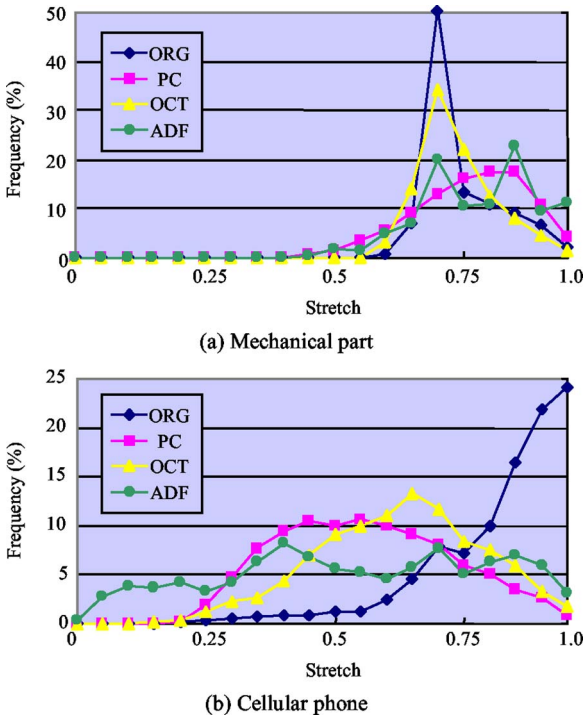

Fig. 15 Stretch distributions

meshers for a simple mechanical part and a front panel of cellular phone. In these examples, we use the high-density meshes generated by meshing of the solid models using an advancing front method as the input of our method. In each figure, (*a*) and (*b*) show the high-density mesh and simplified mesh obtained by our method, and (*c*) and (*d*) show the meshes from finite element meshers. They adopted the octree method and advancing front method, respectively. The numbers of triangular faces and dimensions of each model are shown in Table 2. In Figs. 13 and 14, we can see that our approach generates a mesh visually similar to the finite element mesher's output.

Figure 15 shows the stretch distributions of the meshes shown in Figs. 13 and 14. From these graphs, it was confirmed that our approach could generate a mesh similar to or of better quality than the output of a finite element mesher's outputs. Table 2 shows the results of numerical evaluations of maximum and minimum values of the mesh properties. The results show that our approach could generate a mesh that has controlled limits of face size, stretch and valence by specifying the property control parameters. The existing meshing methods generate highly distorted triangles in the case of a cellular phone. On the other hand, our method can strictly limit minimum stretch of faces larger than 0.2, which is recommended in the commercial finite element solvers [23].

The computation times of MRR generation from high-density meshes of the mechanical part and the cellular phone in Figs. 13 and 14 were about 8 and 19 s, respectively, using a standard personal computer (Pentium Geon 2.4 GHz, RAM 2 Gbyte). In our implementation, the processing times for changing the number of triangular faces using the MRR were less than 1 s in all examples. This means that our method can efficiently generate the meshes suitable for limited computer resources for analysis. We adopted a general data structure for mesh representation and hierarchy representation as a progressive mesh structure [12]. In our implementation, the mesh simplification of a cellular phone model containing one million triangles and the mesh hierarchy representation consumed about 900 M byte memory. In the examples in Tables 1 and 2, much less memory was needed.

6.3 Applications.

6.3.1 Finite Element Analysis. The results of FEA (displacements) using our multiresolution meshes are shown in Fig. 16. Initial meshes are shown in Figs. 8(*b*), 9(*a*), 14(*a*), and by applying our quality improvement method and property control method

Table 2 Mesh information, used parameters and quality[a]

Mesh	Dimension	State[b]	No. of faces	Stretch Ave.	Stretch Min	Valence max	Size max
Mechanical Parts		ORG	45,588	0.767	0.832	9	0.322
	Height 24.4	PC	3,000	0.788	(0.2) 0.357	(10) 10	(4) 3.792
	Width 24.4	OCT	2,970	0.762	0.537	9	3.521
	Depth 48.9	ADF	2,910	0.806	0.492	9	3.757
Cellular phone		ORG	120,186	0.847	0.003	11	1.589
	Height 16.9	PC	16,000	0.586	(0.2) 0.201	(12) 12	(6) 5.859
	Width 49.4	OCT	11,982	0.649	0.054	16	6.681
	Depth 103.3	ADF	13,702	0.558	0.002	11	5.846

[a]Values in parentheses are user-specified parameters in mesh generation.
[b]ORG: original, PC: property controlled, OCT: octree, ADF: advancing front.

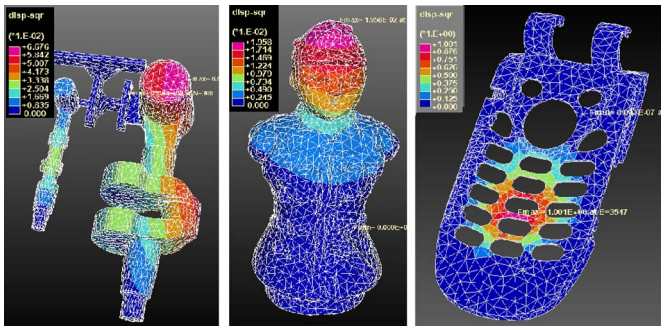

Fig. 16 Results of FEA

to each mesh, the meshes for analysis were obtained. Through applications of our meshes to analysis, it was confirmed that the mesh obtained from RE and tessellations became applicable to the finite element analysis using the proposed method.

6.3.2 Feature Removal for Analysis. In order to perform efficient analysis, removal of small features in the mesh, such as holes, is often required beforehand. The local applicableness of our quality improvement approach allows robust and high-quality feature removal. First, new triangular faces filling the boundary of the hole can be generated without new vertex generation and without consideration of mesh quality. Then by applying a quality improvement method to the new faces locally, high-quality mesh of a feature-removed shape can be obtained. An example of this approach is shown in Fig. 17. In this example, the side faces of the holes were first recognized using simple mesh segmentation [25] and user specification, and they were removed. Then, we applied the simple triangulations to the upper and lower mesh boundaries generated by the side face removals as shown in Fig. 17(*b*), and the local mesh quality improvement for new triangulations was performed as shown in Fig. 17(*b*). By adopting the average face size of the given mesh σ_{Ave} as a subdivision parameter σ_{SZ}, and by introducing a constraint for the face size $\forall f \in f^*(k)$; $Sz(f) \leqslant \sigma_{\mathrm{AVE}}$ in valid edge extraction described in Sec. 4.2.2, quality improvement could be automatically achieved.

7 Conclusions

In this paper, a new scheme for finite element mesh generation from triangular mesh using the multiresolution technique was proposed. Our strategy for changing the properties of mesh was a combination of two processes: a mesh subdivision process to obtain a high-density mesh from a given mesh, and a mesh simplification process to change the mesh properties. Based on this strategy, we proposed two methods for generating the meshes suitable for analysis from various kinds of triangular meshes: a mesh quality improvement method and a mesh property control method. In the mesh quality improvement method, mesh subdivision based on midpoint insertions for increasing the DOF of mesh connectivity manipulation, and simplification using edge collapse based on quality improvement metric could achieve robust and effective mesh quality improvement for several kinds of low-quality meshes. Also in the mesh property control method, as in the quality improvement, uniform subdivision, and mesh simplification with property control using user-specified parameters could generate property controlled mesh suitable for finite element analysis. Through numerical evaluations, it was confirmed that our approach could achieve robust and effective high-quality and property-controlled mesh generation for different kinds of meshes obtained from tessellation, RE, mesh combining and finite element meshers. Also the applicableness of our approach to finite element analysis and feature removal for analysis was shown.

Our future works are as follows: Analysis accuracy verification, local resolution control according to the results of analysis or user-requirements, extension of our method to assembly models considering contact face correspondence and to tetrahedral (volume) mesh generation based on volume mesh simplifications [26].

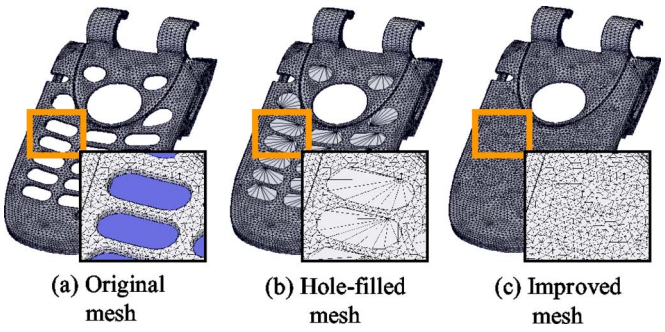

Fig. 17 An example of hole filling

Acknowledgment

This work was financially supported by the grant-in-aid of Intelligent Cluster Project (Sapporo IT Carrozzeria) founded by MEXT.

References

[1] Owen, S. J., 1998, "A Survey of Unstructured Mesh Generation Technology," *Proc. 7th International Meshing Roundtable*, Dearborn, Michigan, pp. 239–267.
[2] Topping, R. H. V., Muylle, J., Iványi, P., Putanowiez, R., and Cheng, B., 2004, *Finite Element Mesh Generation*, Saxe-Couburg Publications, Kippen, Chap. 3.
[3] Shimada, K., and Gossard, D. C., 1995, "Bubble Mesh: Automated Triangular Meshing of Non-Manifold Geometry by Sphere Packing," *Proc. ACM Symposium on Solid Modeling and Applications*, ACM, pp. 409–419.
[4] Bechet, E., Cuilliere, J. C., and Trochu, F., 2002, "Generation of a Finite Element MESH from Stereolithography (STL) Files," Comput.-Aided Des., **34**, pp. 1–17.
[5] Bianconi, F., 2002, "Bridging the Gap between CAD and CAE using STL Files," International Journal of CAD/CAM, **2**(1), pp. 55–67.
[6] Floater, M. S., 1997, "Parameterization and Smooth Approximation of Surface Triangulations," Comput. Aided Geom. Des., **14**(3), pp. 231–250.
[7] Sheffer, A., and Sturler, E., 2001, "Parameterization of Faceted Surfaces for Meshing using Angle-based Flattening," Eng. Comput., **17**(3), pp. 326–337.
[8] Alliez, P., Meyer, M., and Desbrun, M., 2002, "Interactive Geometry Remeshing," *Proc. SIGGRAPH'02*, ACM Press, New York, pp. 347–354.
[9] Stollnitz, E. J., DeRose, T. D., and Salesin, D. H., 1996, *Wavelets for Computer Graphics: Theory and Application*, Morgan Kaufmann, San Francisco, Chap. 10.
[10] Sifri, O., Sheffer, A., and Gotsman, C., 2003, "Geodesic-based Surface Remeshing," *Proceedings of the 12th International Meshing Roundtable*, Santa Fe, New Mexico, pp. 189–199.
[11] Garland, M., and Heckbert, P. S., 1997, "Surface Simplification Using Quadric Error Metrics," *Proceedings of the SIGGRAPH'97*, ACM Press, New York, pp. 209–216.
[12] Hoppe, H., 1996, "Progressive Meshes," *Proceedings of the SIGGRAPH'96*, ACM Press, New York, pp. 98–108.
[13] Luebke, D., Reddy, M., Cohen, J. D., Varshney, A., Watson, B., and Huebner, R., 2003, *Level of Detail for 3D Graphics*, Morgan Kaufmann, San Francisco.
[14] Taubin, G., Guéziec, A., Hom, W., and Lazarus, F., 1998, "Progressive Forest Split Compression," *Proceedings of the 25th Annual Conference on Computer Graphics and Interactive Techniques*, ACM Press, New York, pp. 123–132.
[15] Karabassi, E. A., Papaioannou, G., Fretzagia, C. and Theoharis, T., 2003, "Exploiting Multiresolution Models to Accelerate Ray Tracing," Comput. Graphics, **27**, pp. 91–98.
[16] Floriani, L. D., Magillo, P., Morando, F., and Puppo, E., 2000, "Dynamic View-Dependent Multiresolution on a Client-Server Architecture," Comput.-Aided Des., **32**, pp. 805–823.
[17] Fine, L., Remondini, L., and Leon, J. C., 2000, "Automated Generation of FEA Models through Idealization Operators," Int. J. Numer. Methods Eng., **49**, pp. 83–108.
[18] Loop, C., 1987, "Smooth Subdivision Surfaces based on Triangles," Master thesis, University of Utah.

[19] Zorin, D., and Schröder, P., 2000, "Subdivision for Modeling and Animation," SIGGRAPH2000 Course Notes, 36.
[20] Yau, H., T., Kuo, C. C., and Yeh, C. H., 2003, "Extension of Surface Reconstruction Algorithm to the Global Stitching and Repairing of STL Models," Comput.-Aided Des., **35**, pp. 477–486.
[21] Ju, T., 2004, "Robust Repair of Polygonal Models," *Proceedings of the SIGGRAPH2004*, ACM, New York, pp. 888–895.
[22] Page, D. L., Sun, Y., Koschan, A. F., Paik, J., and Abidi, M. A., 2002, "Normal Vector Voting: Crease Detection and Curvature Estimation on Large, Noisy Meshes," Graphical Models, **64**, pp. 199–229.
[23] *IDEAS users manual*, 2003.
[24] Kanai, T., Suzuki, H., and Kimura, F., 2000, "Metamorphosis of Arbitrary Triangular Meshes," IEEE Comput. Graphics Appl., **20**(2), pp. 62–75.
[25] Date, H., Kanai, S., Kishinami, T., Kobayashi, M., and Iwakoshi, M., 2004, "A Prototyping System for Surface Textured Shapes using Triangular Mesh Modeling and Stereo Lithography," *Proceedings of the 2004 Japan-USA Symposium on Flexible Automation*, Denver, Colorado, Paper No. JL018.
[26] Staadt, O. G., and Gross, M. H., 1998, "Progressive Tetrahedralizations," *Proceedings of the Conference on Visualization 98*, IEEE Computer Society Press, Washington, pp. 397–402.